Carbohydrate Polymers 92 (2013) 612–620

Contents lists available at SciVerse ScienceDirect

Carbohydrate Polymers

journal homepage: www.elsevier.com/locate/carbpol

Bioactive glasses-incorporated, core–shell-structured polypeptide/polysaccharide nanofibrous hydrogels

Jian Chen[a], Xiaoyi Chen[b], Xianyan Yang[b], Chunmao Han[a], Changyou Gao[b,c], Zhongru Gou[b,*]

[a] Department of Surgery, The 2nd Affiliated Hospital, Zhejiang University of School of Medicine, Hangzhou 310009, China
[b] Zhejiang-California International NanoSystems Institute, Zhejiang University, Hangzhou 310029, China
[c] MOE Key Laboratory of Macromolecular Synthesis and Functionalization, Department of Polymer Science and Engineering, Zhejiang University, Hangzhou 310027, China

ARTICLE INFO

Article history:
Received 20 May 2012
Accepted 15 September 2012
Available online 3 October 2012

Keywords:
Gelatin nanofiber
Inorganic–organic hybrid
Polysaccharides
Biomimetic hydrogels

ABSTRACT

Although the synthetic hydrogel materials capable of accelerating wound healing are being developed at a rapid pace, achieving inorganic–organic hybrid at nanoscale dimension in nanofibrous hydrogels is still a great challenge because of its notorious brittleness and microstructural stability in wet state. Here, we developed a new nanofibrous gelatin/bioactive glass (NF-GEL/BG) composite hydrogel by phase separation method and followed by arming the nanofibers network with counterionic chitosan–hyaluronic acid pairs for improving microstructural and thermal integrity. We achieve this feature by carrying an optimal balance of charges that allows the inorganic ion release in aqueous solution without minimal structure collapse. Therefore, such NF-GEL-based, polysaccharide-crosslinked bioactive hydrogel could afford a close biomimicry to the fibrous nanostructure and constituents of the hierarchically organized natural soft tissues to facilitate chronic, nonhealing wound treatment.

1. Introduction

Synthetic hydrogels, cross-linked materials that typically consist of over 50% water, are notoriously brittle and have poor microstructural and mechanical stabilities (Tanaka, Gong, & Osada, 2005). Considerable efforts have been recently made to develop advanced polypeptide- and/or polysaccharide-based nanofibrous hydogel for enhancing wound repair (Guo et al., 2009; Jonker, Lowik, & van Hest, 2012). In wound operations, the purpose of dressing the wound is to promote an optimal healing environment by providing pain relief, protection from trauma and infection, a moist environment, and removal of debris. By simultaneously maximizing the patient's nutritional status and providing meticulous wound care, most wounds will heal appropriately (Lewis, Whitting, ter Riet, O'Meara, & Glanville, 2001). However, when the wound tissue is edematous and/or nonhealing because of severe tissue damage, poor blood flow, inflammation and infection, repair by conventional wound dressing and antibiotic administration may become technically unreliable and compromise wound healing (Boatenog, Matthews, Stevens, & Eccleston, 2008; Brem et al., 2003). Chronic, nonhealing wounds are involved progressively more tissue loss and bacterial colonization, particularly in venous stasis, diabetic ulcer, and bed sores, and thus give rise to the biggest challenge to wound-care hydrogel researchers (Ehrenreich & Ruszczak, 2006; Gurtner, Werner, Barrandon, & Longaker, 2008).

Multiple studies have shown that the local release of some inorganic ions from wound dressings can suppress microoganisms and accelerate wound repair process (Ali, Rajendran, & Joshi, 2011; Kawai et al., 2011; Neel, Ahmed, Pratten, Nazhat, & Knowles, 2005; Youk, Lee, & Park, 2004; Xu & Zhou, 2008). The ionic form of silver (Ag^+) is a well-known highly antibacterial material, and the silver-loaded dressing is an increasingly popular approach in the control of wound bioburden (Ali et al., 2011). However, a high concentration of silver impairs the functioning of the central and peripheral nervous systems (Chopra, 2009; Leaper, 2006). It is well recognized that calcium is an important factor in the wound healing of skin and suspect that it is required for the migration of epidermal cells (Lansdown, 2002). Clinically, the direct topical application of calcium to chronic wounds through calcium alginate dressings has been shown to be beneficial (Motta, 1989). Recently, it has been found that some bioactive glasses (BGs) readily form a soft tissue bond and their ion release products stimulate collagen production (Hench, 2006). Wilson, Pigott, Schoen, and Hench (1981) firstly showed that soft connective tissues could form a bond to 45S5 Bioglass® and established the safety of use of particulate forms in soft tissue if the interface was immobile. More recent studies demonstrated the beneficial effects of 45S5 and borate containing

* Corresponding author at: Zhejiang-California International NanoSystems Institute, Zhejiang University, Kaixuan Road 268, Hangzhou 310029, China.
Tel.: +86 571 8697 1782; fax: +86 571 8697 1539.
E-mail address: zhrgou@zju.edu.cn (Z. Gou).

0144-8617/$ – see front matter © 2012 Elsevier Ltd. All rights reserved.
http://dx.doi.org/10.1016/j.carbpol.2012.09.030

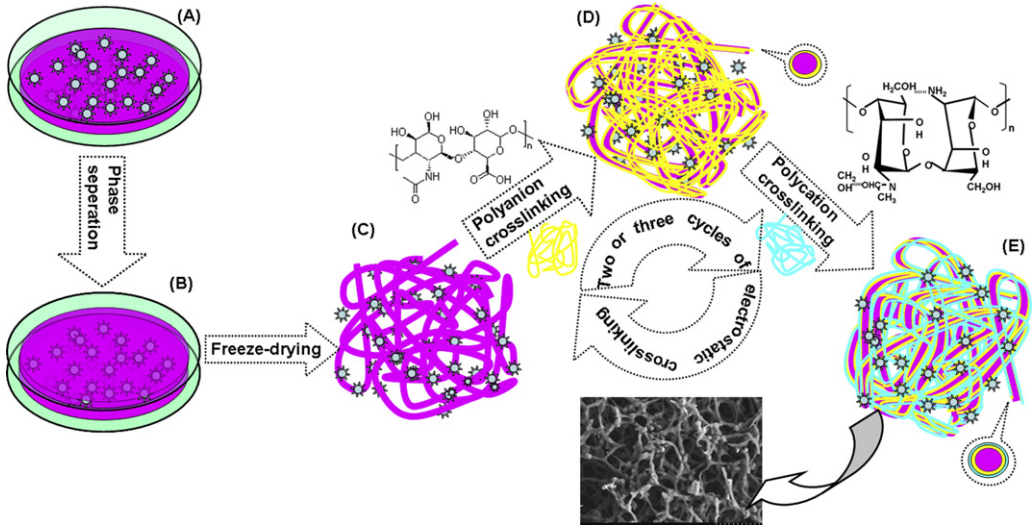

Scheme 1. Experimental procedure for preparing the nanofibrous organic–inorganic hybrid hydrogels via phase separation (A and B) and fabricating core–shell-structured nanofibrous polypeptide–polysaccharide composite hydrogels via electrostatic crosslinking (C–E).

13–93 BGs to promote angiogenesis, which is critical to the healing of soft tissue wounds (Gorustovich, Perio, Roether, & Boccaccini, 2010; Rahaman et al., 2011). Thus, the development of BG-loaded hydrogels with antimicrobial activity is highly desired.

The biomimetic biopolymeric nanofiber hydrogels closely mimic the microstructure and porosity of extracellular matrices (ECMs) in which growth factors, drugs and nutrients freely diffuse in scaffolds at very slow rates (Van Vlierberghe, Dubruel, & Schacht, 2011). Among the preparation methods, the self-assembling peptide nanofiber hydrogels are of particular interest due to the attractive extracellular matrice-mimicking porous architecture which may promote wound healing, skin regeneration and enhance angiogenics (Sun et al., 2011; Schneider, Garlick, & Egles, 2008). Unfortunately, the self-assembly methods usually require multiple labor-intensive steps associated with peptide preparation and purification, and slow assembly in specific electrolyte environment (Hartgerink, Elia, & Stupp, 2002; Zhang, Gelain, & Zhao, 2005). Furthermore, these procedures are not enough to meet the scalable yield for wound management, and maybe result in instable individual fibrous structure when incorporating with dissolvable particles. Electrospinning has been studied widely because of its efficiency and simplicity in fabricating of nanofibrous structures. Natural polymers such as gelatin (GEL) (Rujitanaroj, Pimpha, & Supaphol, 2008), chitosan (CS) (Tchemtchoua et al., 2011), and hyaluronic acid (HA) (Li et al., 2006; Uppal, Ramaswamy, Arnold, Goodband, & Wang, 2011) have been used to produce nanofibrous hydrogel mats as bioactive dressings. However, the usage of cytotoxic solvents, the size limitation of inorganic particles, three-dimensional (3D) structure maintenance, and limited spinnable conditions are all drawbacks in organic–inorganic hybrid electrospinning (Xie, Li, & Xia, 2008). On the other hand, some nanofibrous hydrogel's capacity to act as the porous matrices of BG microparticles for wound care is limited due to its poor mechanical and thermal stabilities at physiological temperature, and particularly the conventional chemical crosslinking make the hydrogels bind tissue rapidly and tightly, which is catastrophic to skin wound treatment (Liang, Chang, Liang, Lee, & Sung, 2004). Thus a further challenge in the design of bioactive dressings is how to produce scalable biomimetic nanofibrous hydrogels for accelerating the chronic wound healing, without involving environmentally/biologically harmful additives or inert materials.

Herein we developed a reliable, facile way to fabricate the novel GEL/BG@CS–HA hydrogels based on thermally induced phase separation and electrostatic crosslinking techniques, which would create stable nanofibrous 3D porous architecture and integrate the antibacterial and bioactive properties (Scheme 1). This method may be easily scaled-up to prepare large quantities of BG-incorporated core–shell nanofibers with GEL as core and CS–HA complex as shell. The superb structural and thermal integrity and chemically tunable bioactivity and antimicrobial activity provide tremendous opportunities for their use as an efficient wound dressing in non-healing wounds.

2. Materials and experiment

2.1. Chemicals and materials

High-purity grade inorganic salts, GEL (type B, from bovine skin), trishydroxymethyl aminomethane (Tris), and ethanol (≥99.8 wt.%) were purchased from Sinopharm Chemical Reagent Co. Ltd., CS ($M_W \sim 50$ kDa; degree of deacetylation: 85%; Shandong Haidebei Marine Bioengineering Co. Ltd.), Tris(hydroxyllmethyl) aminomethane (Tris; Bio-Rad), and HA (Freda Biochem Co. Ltd.) were used as received. Ultrapure MiniQ water (18.2 MΩ cm^{-1}) was used in experiments. The 45S5 BG particles (with similar composition to Biolgass® 45S5) were prepared by a sol–gel method with chemical composition (wt.%): 45.0 SiO_2, 24.5 CaO, 24.5 Na_2O, and 6 P_2O_5 as reported previously (Chen & Thouas, 2011).

2.2. Preparation of conventional GEL/BG composites

GEL (6.0 g) was dissolved in 120 mL deionized water at 50 °C to make a GEL solution of 5.0% (w/v). Then, the solution was divided into six equal parts (20 mL) and added 0, 4, 8, and 12 mg BG powders under magnetic stirring to for mixture solutions with BG/GEL mass ratio of 0, 0.4%, 0.8%, and 1.2%, respectively. The GEL solutions were added into the 6-well cell culture plates (CCP) and were kept at −80 °C for 24 h. After that, the frozen gels were lyophilized for 48 h. The dried GEL/BG porous composites were stored in a desiccator until characterization.

2.3. Preparation of nanofibrous GEL/BG porous composites

Gelatin was dissolved in 50/50 (v/v) ethanol/water mixture at 55 °C to make a GEL solution of 5.0% (w/v). Under continuous stirring, the 0, 4, 8, and 12 mg BG powders were added into 20 mL

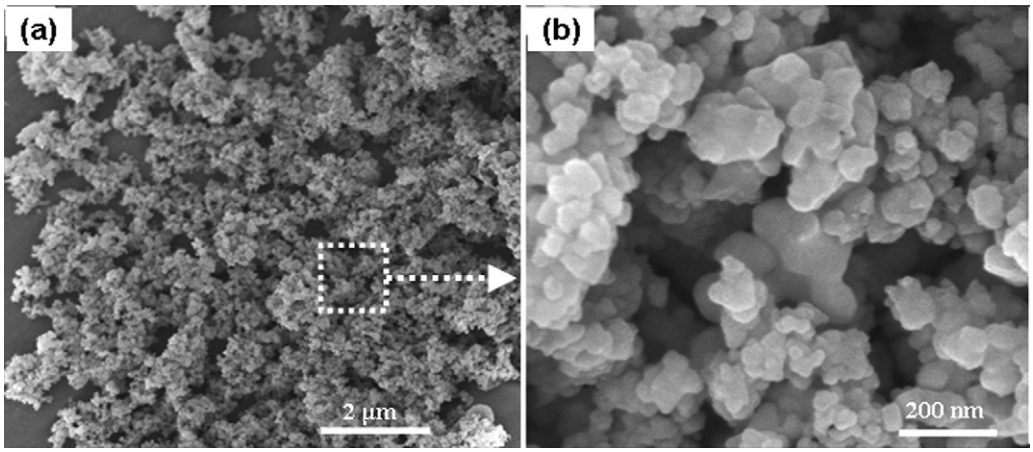

Fig. 1. SEM image of the as-calcined 45S5 BG particles via sol–gel method.

solution, respectively. The GEL/BG solution (20 mL) was added into three pore of CCP and was phase separated at −80 °C for 24 h. The frozen gel was firstly immersed into cold ethanol (−18 °C) for 6 h, and then lyophilized for 36 h or over to produce nanofibrous GEL/BG (NF-GEL/BG) sponge. The NF-GEL/BG sponges were cut into samples with a thickness of 3.0 and 5.0 mm for microstructure observation or use. A similar procedure was used to prepare NF-GEL/BG sponges except that the ethanol/water ratio ranged from 10/90 to 40/60 (v/v).

2.4. Electrostatic crosslinking of NF-GEL/BG composites

Electrostatic crosslinking of 3D NF-GEL/BG composites (5.0 mm in thickness) with 0.3 wt.% HA and 0.6 wt.% CS solutions was carried out under high vacuum condition, respectively. To maintain the nanofibrous morphology and prevent their microstructure collapse in aqueous environment, the organic–inorganic hybrid sponges were outgassed and infiltrated in HA solution (an air pressure <5 mmHg) at 4 °C for 5 min. Then, the vacuum was released and the sponges were washed in MiniQ water (∼10 °C) for one minute to leach out HA in the sponge surface layer. A similar procedure was used to infiltrate in CS solution and immersed under the same conditions. More counterionic polysaccharides were coated by increasing the crosslinking cycles while the other conditions remained the same. Finally, the FN-GEL/BG@HA–CS sponges were lyophilized for 36 h and stored in a desiccator for microstructure characterization using digital camera (Nikon) and scanning electron microscopy (SEM; HITACHI, S4800). Gold sputtering was used prior to SEM observation.

2.5. Equilibrium water uptake capacity (WUC) and volume change ratio (VCR) measurement

The swelling ratio of sponges was determined by immersing the porous sponges in MiniQ water at 37 °C for 24 h and was considered to reach the equilibrium of water uptake. The WUC and VCR were quantified as: WUC (wt.%) = $(W - W_0)/W_0 \times 100$ and VCR (v/v%) = $V_s/V_d \times 100$, where W_0, W are the dry weight and wet weight of the specimens before and after immersing in MiniQ water and removing the surface water with filter paper; V_d, V_s are the original volume of specimens and the measured volume of swelled sponges after immersing in MiniQ water, respectively.

2.6. Inorganic ion release in vitro and ICP analysis

The inorganic ion release was investigated for the FN-GEL/BG@HA–CS sponges (500 mg) (5.0 mm in thickness) by immersing in 20 mL Tris buffer (0.02 M) with an initial pH 7.40 at physiological temperature in vitro. After immersing for different time intervals, changes in pH of aqueous medium were measured firstly; then 2.0 mL of supernatant was diluted in 5% HCl solution prior to inductively coupled plasma (ICP; Thermo) analysis, and aliquot amount of fresh buffer (2 mL) was added into the buffers to maintain the solution volume constant. The as-immersed sponges for 24 h were kept at −20 °C for 4 h and then lyophilized for SEM observation.

3. Results and discussion

3.1. SEM observation of BG particles

Sol–gel method is versatile to prepare nanoscale BG powders after the low-temperature calcination treatment. The sol–gel-derived 45S5 BG powders exhibited very low aggregation, with one to two hundred nanometer in dimension (Fig. 1). The measured composition of particles was 46.7 mol.% SiO_2, 26.3 mol.% CaO, 23.5 mol.% Na_2O, and 3.5 mol.% P_2O_5, similar to the theoretical values reported previously (Wilson et al., 1981).

3.2. GEL/BG hybrid sponges via conventional freeze-drying and phase separation techniques

The pure GEL solution is usually in a hydrosol state at above physiological temperature. When GEL concentration is high enough and its temperature is decreased to below 37 °C, the hydrosol transform into hydrogel. Thus the pure GEL porous sponge, with a considerable volume shrinkage (∼70%), could be obtained by freeze-drying its hydrosol. It was evident that the GEL sponge was composed of closed pores with tens of micron in size, and the pore wall was made of thin smooth plates (Fig. 2a and b). With increasing BG/GEL ratio from 0.4% to 1.2% in the hybrid hydrosol, the BG particles could be seen in the pore walls, and was prone to aggregation (Fig. 2c–l).

The GEL/BG hybrid sponges with BG/GEL ratio of 1.2% via thermal induced phase separation processing in ethanol/water solvent mixture showed significant difference on the pore wall with increasing ethanol concentration from 10% to 40% (Fig. 3). There grew some short fiber-like floccules on the pore wall. With the ethanol concentration increased up to 50%, the porous sponges had a limited volume shrinkage (<10%) (Fig. 4a), and particularly the architecture of the GEL matrices was a 3D continuous fibrous network (Fig. 4b–e). The BG particles were anchored in the NF-GEL matrix, without any aggregation. It should be noted from the

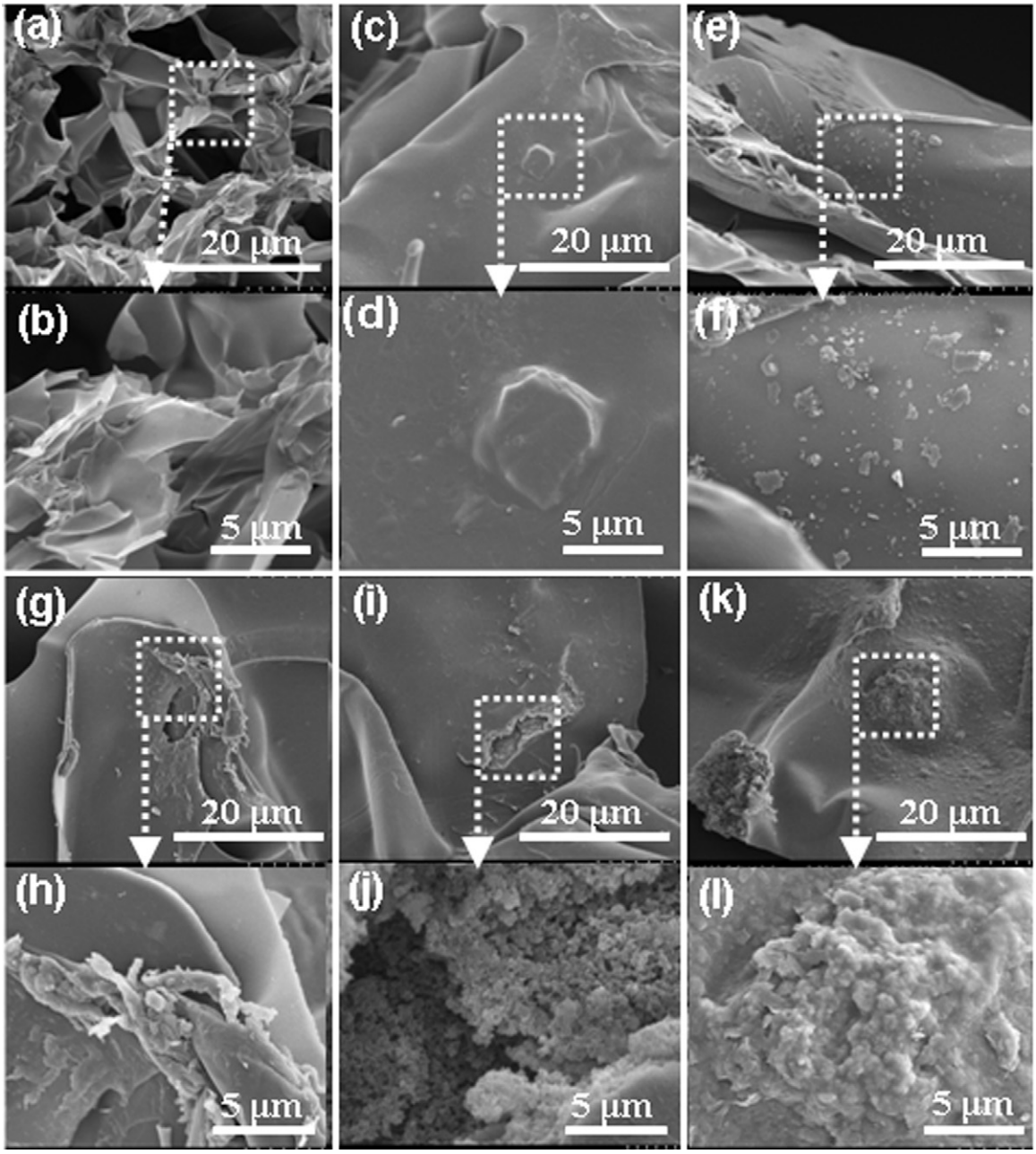

Fig. 2. SEM image of the conventional GEL/BG hybrid sponges with BG/GEL ratio of 0 (a and b), 0.4% (c and d), 0.6% (e and f), 0.8% (g and f), 1.0% (i and j) and 1.2% (k and l) via direct freeze-drying method.

cross-sectional observation (Fig. 4f–h) that the BG particles exhibited graded distribution, but the GEL fiber diameter ranged from tens to hundred of nanometers, which was the same range as that of natural collagen matrices.

3.3. FN-GEL/BG@HA–CS nanofiber sponges via electrostatic crosslinking treatment

In order to maintain the structural integrity of NF-GEL/BG architecture because GEL can readily swell in physiological fluid, an oppositely charged polyelectrolyte crosslinking technique was introduced during NF-GEL/BG sponge post-processing. The dilute solution of two counterionic polysaccharides, i.e., HA and CS, were used to infiltrated the NF-GEL/BG sponges under high vacuum condition. According to the SEM observation, when the polysaccharide-infiltrated FN-GEL/BG sponges were directly lyophilized without undergoing MiniQ water washing for 2 min, the sponge surface layer also produced smooth wall plates (Fig. 5a and b), similar to that prepared by conventional freeze-drying method. In contrast, the water-washed, polysaccharide-crosslinked sponges maintained the fibrous structure (Fig. 5c and d). The BG particles were coated and scarcely naked in the fiber with an increasing crosslinking cycles of HA–CS pairs, and especially new joint welding of the fibers at their neighboring points and their cross-points was observed. However, there had little difference in appearance after the sponges underwent one and two cycles of HA–CS coating (Fig. 5c and d, insets). Interestingly, many fibrous structures could be maintained for the FN-GEL/BG@HA–CS sponges after immersion in Tris buffer for 24 h (Fig. 5e and f).

Table 1 listed the WUC and VCR which had similar trends with increasing the oppositely charged HA–CS crosslinking cycles. The sample with highest BG/GEL ratio (1.2%) after one time

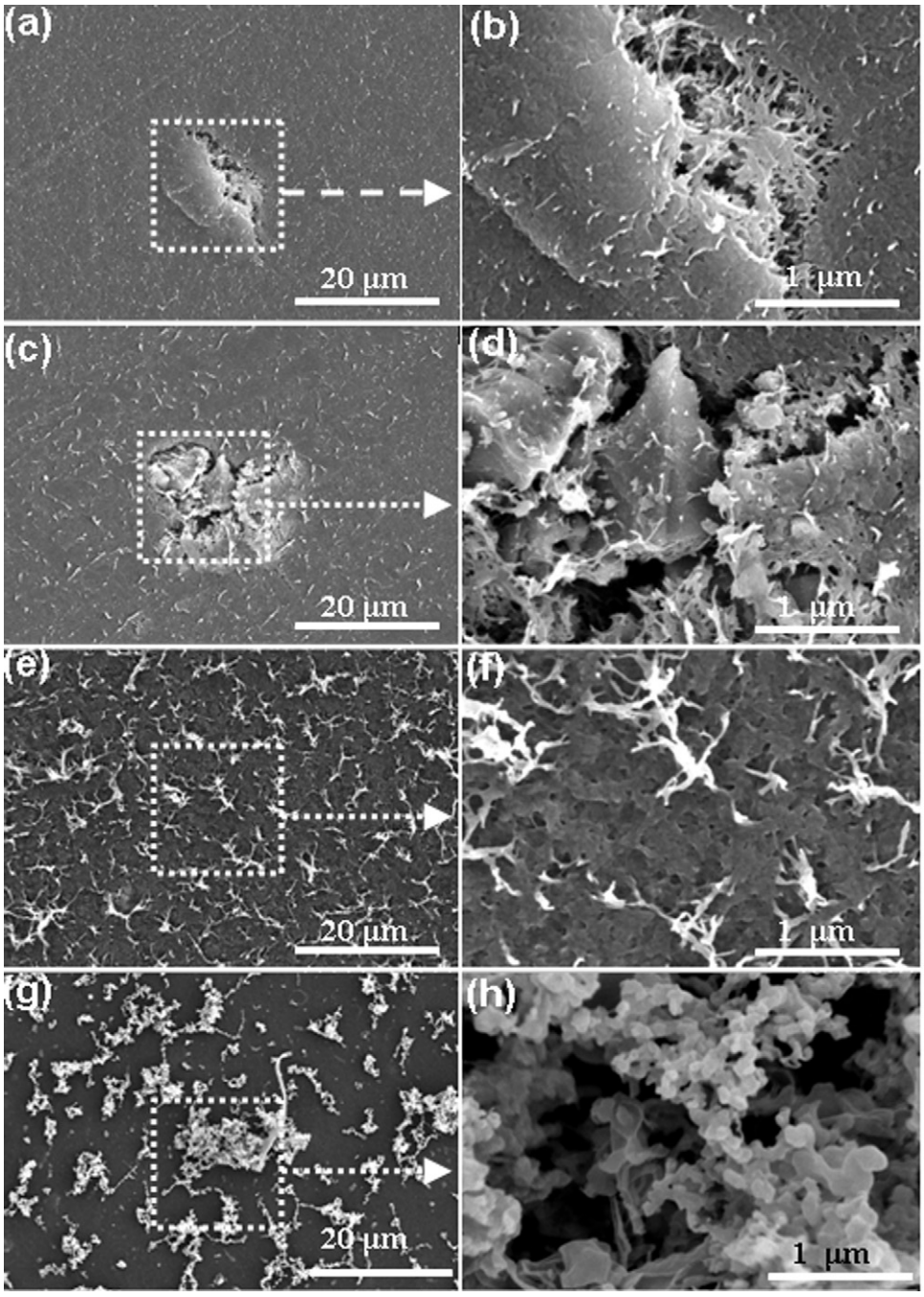

Fig. 3. SEM micrographs of the GEL/BG hybrid sponges via thermal induced phase separation processing in ethanol/water solvent mixture with ethanol concentration of 10% (a and b), 20% (c and d), 30% (e and f) and 40% (g and h), respectively.

of HA–CS treatment had the highest (903.3 ± 43.2%), its VCR was 143.0 ± 15.6% (v/v). In contrast, the WUC and VCR of the sponge with lowest BG/GEL ratio (0.4%) reduced, respectively, to 695.2 ± 33.4% and 116.2 ± 11.8% (v/v) after three times of HA–CS crosslinking. These results suggest that the crosslinked sponges become more rigid and less hydrophilic because GEL has higher hydrophilicity, but the incorporation of BG in the polymer matrix readily enhance its water uptake capacity.

Table 1
Gel properties of FN-GEL/BG@HA–CS hydrogels with the variation of the BG/GEL mass ratio (0.4%, 0.8%, and 1.2%) and electrostatic crosslinking cycles.

Crosslinking cycle	Water uptake capacity (w/w%)			Volume change ratio (v/v%)		
	0.4%	0.8%	1.2%	0.4%	0.8%	1.2%
1	840.2 ± 38.3	882.1 ± 31.8	903.3 ± 43.2	134.3 ± 12.6	139.3 ± 13.6	143.0 ± 15.6
2	742.5 ± 46.6	776.6 ± 27.8	819.0 ± 42.7	122.6 ± 11.5	126.6 ± 13.1	128.6 ± 14.8
3	695.2 ± 33.4	723.3 ± 41.0	752.4 ± 24.2	116.2 ± 11.8	120.5 ± 14.6	123.6 ± 13.7

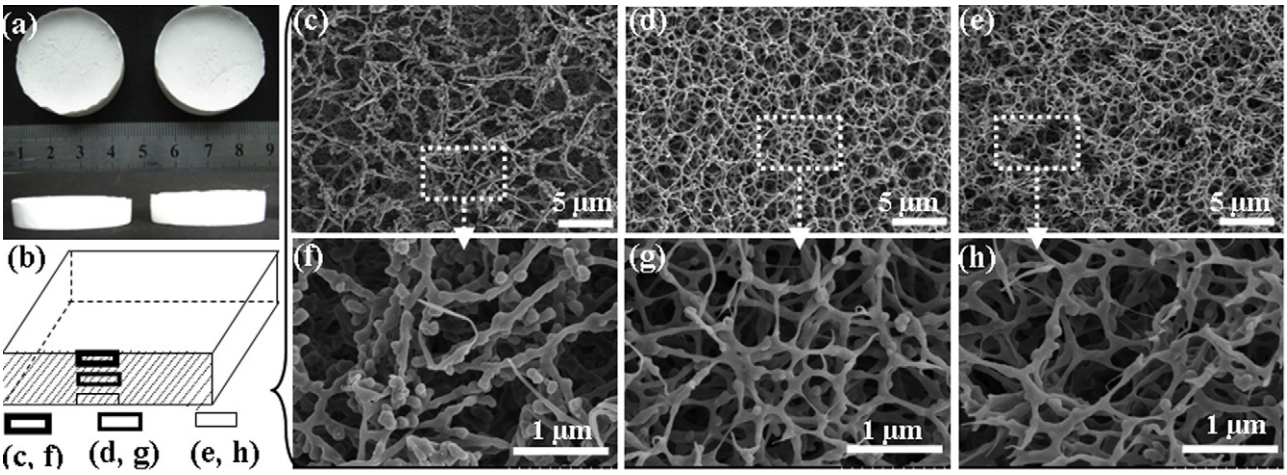

Fig. 4. Digital images of the FN-GEL/BG@HA–CS sponges (a) and the schematically selected cross-sectional zones (b) for the microstructure by SEM observation (c–h) of the representative sample.

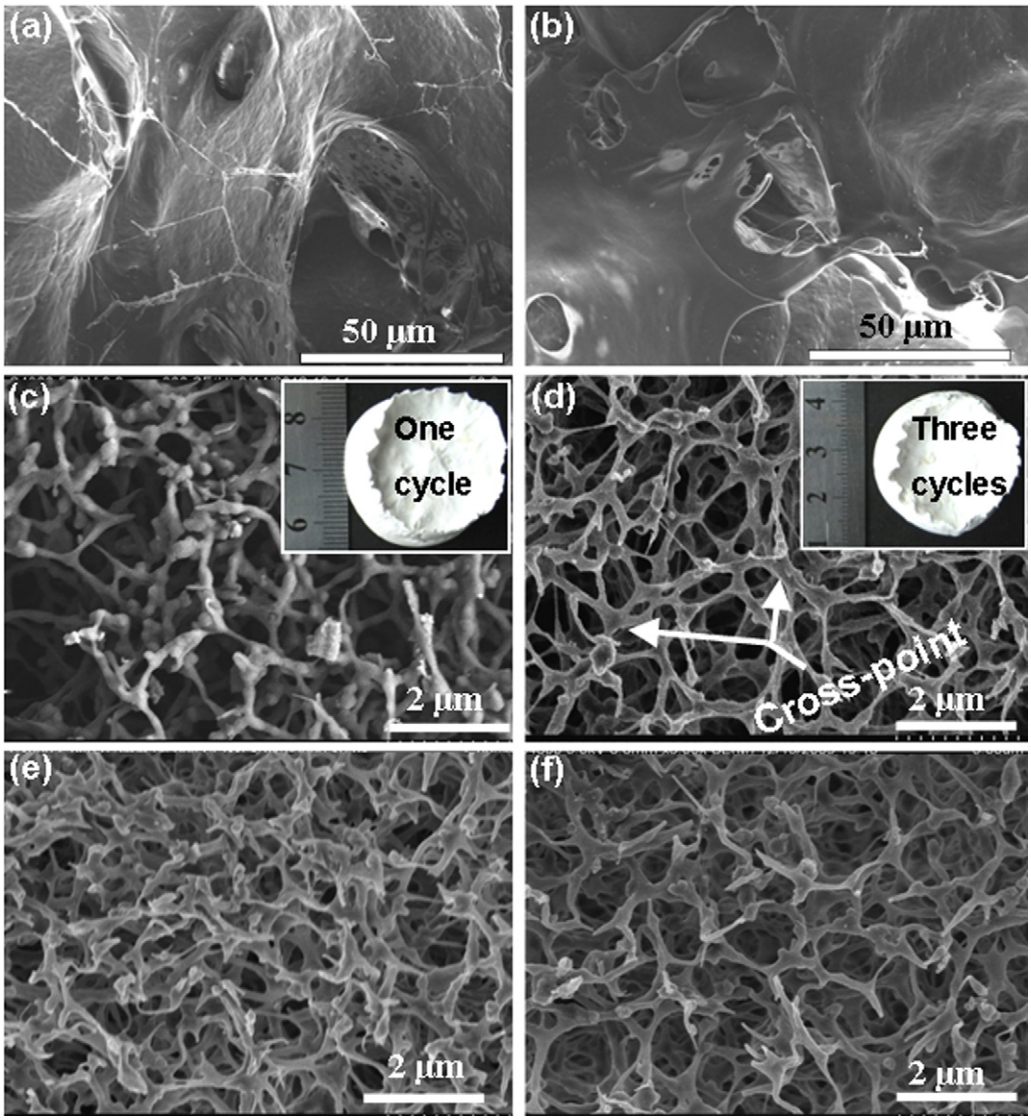

Fig. 5. The surface microstructure (SEM images) of the directly lyophilized, HA- (a) or CS- (b) crosslinked FN-GEL/BG sponges without water washing, and the representative SEM micrographs of water-washed FN-GEL/BG@HA–CS sponges via one or three cycles of crosslinking (c and d) and immersing in Tris buffer for 24 h (e and f). The arrows indicate welding at the cross-points. Insets in (c and d) represent the outward of the sponges after one or three cycles of crosslinking treatment.

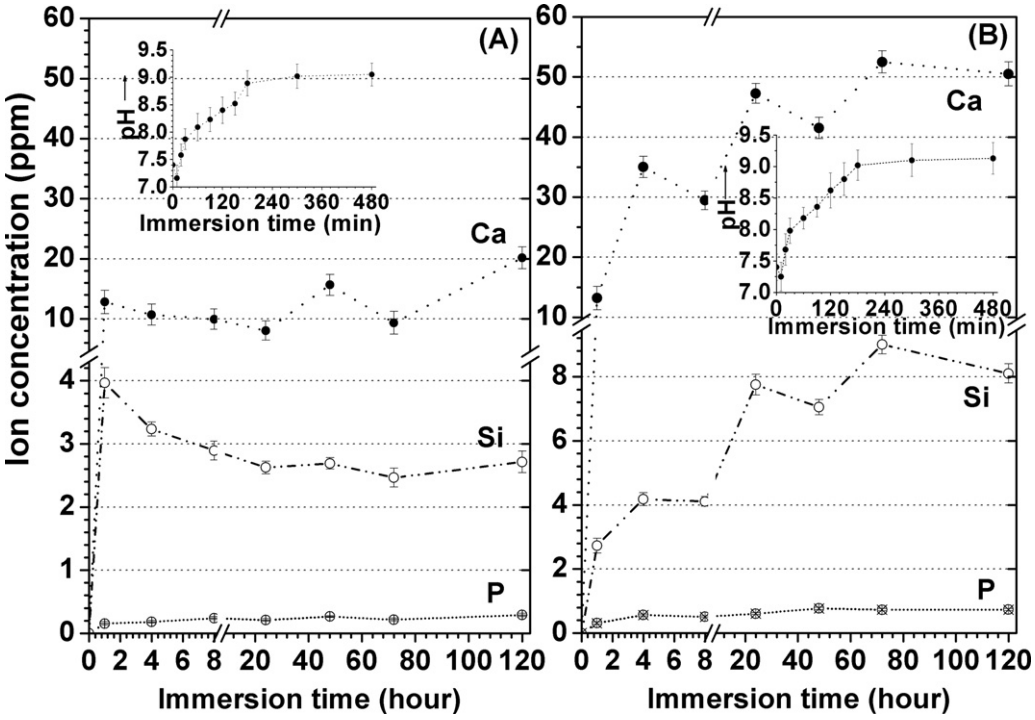

Fig. 6. Changes in inorganic ion concentrations in the buffer media during immersing the FN-GEL/BG@HA–CS sponges with BG/GEL ratio of 0.4% (a) and 1.2% (b), respectively.

3.4. Ion release behavior from FN-GEL/BG@HA–CS nanofiber sponges

To distinguish the contribution of BG content for the inorganic ion release, different immersion times, the FN-GEL/BG@HA–CS sponges with BG/GEL ratio of 0.4% and 1.2% immersed in Tris buffer 37 °C were investigated. Fig. 6 shows that the rapid calcium and silicon accumulation took place in the aqueous media within the initial 4 h, accompanying with a slow release of phosphorus. In particular, the calcium and silicon concentrations for the sample with 1.2% BG/GEL ratio (Fig. 6b) were over three-fold and two-fold higher for the sample with 0.4% BG/GEL ratio (Fig. 6a) after immersion for 24 h, indicating the inorganic ion dose in the immersion media can be adjusted by changing the BG content in the hybrid sponges. Indeed, the overall concentrations of sodium ions increased markedly from the initial zero to nearly 1.5-fold of calcium ions in the media within 4 h, and thereafter kept stable without much fluctuation (data not shown). In addition, the pH of the immersion solutions increased markedly from the initial value of 7.4 up to 8.2 or over within 60 min (Fig. 6, insets). Although the values varied depending on the BG content, similar trends in pH change were observed for two kinds of samples. The greatest rate of pH increase was recorded within the first 120 min, and within 180–300 min the maximum level (pH ~ 9.1) was reached, which would be effective in inhibiting the growth of some bacteria.

Until now, many researchers have examined GEL, HA, CS, and BG, respectively, as promising materials for the acceleration of wound healing (Chang, Chang, Lai, & Sung, 2003; Gillette, Swaim, Sartin, Bradley, & Coolman, 2011; Tran, Joung, Lih, & Park, 2011; Uppal et al., 2011). GEL is available via a controlled hydrolysis of collagens, which is one of the most abundant structural fibrous insoluble proteins throughout body. Unfortunately, GEL exhibits poor mechanical stability that is too brittle when fully dried or too soft when fully wet and is easily soluble in aqueous medium. The gelation temperature of GEL is very close to the human physiological temperature, and accordingly the GEL-based dressings must be crosslinked to improve its thermal and structural stabilities in the wet state. The water-soluble genipin and carbodiimide are attractive crosslinkers to date to overcome the cytotoxicity problem associated with the formaldehyde-crosslinked GEL hydrogels (Fujikawa, Fukui, & Koga, 1987; Liang et al., 2004; Sung, Huang, Chang, Huang, & Hsu, 1999). Fujikawa et al. (1987) pointed out that genipin can react spontaneously with free amino groups of lysine or hydroxyline residues within collage-based biomaterials. However, the genipin- and carbodiimide-crosslinked GEL hydrogels are viscous and readily stick close to the surface of a lesioned wound (Sung et al., 1999).

The primary objective of this study is to develop a NF-GEL-based hydrogel dressing with improved bioactivity and antibacterial. Recent studies have demonstrated the angiogenic effects of BG, i.e., increased secretion of vascular endothelial growth factors (VEGFs) and VEGF gene expression in fibroblasts, the proliferation of endothelial cells and formation of endothelial tubules in vitro, as well as enhancement of vascularization in vivo (Gorustovich et al., 2010). Moreover, BGs may inhibit the growth of a wide selection of aerobic and anaerobic bacterial species typically causing infections on the surface of prostheses, and the antibacterial activity of BG correlated mainly with the ion doping, particle size, pH and high silicon ion levels in the supernatant (Xie et al., 2009; Waltimo, Brunner, Vollenweider, Stark, & Zehnder, 2007). Zhang et al. studied the dissolution behavior of six BGs containing no special antibiotic ion with their antibacterial effects against sixteen clinically important bacterial species. Their studies showed that the rapid dissolution of the glasses leading to increase in pH and ionic concentration was assumed to give the antibacterial effects (Zhang et al., 2010). Therefore, the incorporation of BG into NF-GEL dressing is highly desirable and beneficial for improving the chronic, nonhealing wound treatment.

On the other hand, the post-processing method using highly biocompatible HA–CS pair is selected as our choice of an electrostatic crosslinking technique as it has many advantages over the conventional chemical crosslinking. HA, as a highly hydrated anionic polysaccharide, is found an essential component from the vitreous of the eye to the ECMs of cartilage, in which its structural and

biological properties is much favorable to accelerating wound repair (Burdick & Prestwich, 2011). CS is obtained by the hydrolysis of chitin and is the only cationic polysaccharide in nature, with outstanding wound healing effect, antimicrobial activity, and tissue anti-adhesion nature (Muzzarelli, 2009). Thus it can be assumed that the bioactive potential of FN-GEL/BG@HA–CS hybrid hydrogels can be attributed two aspects: the inorganic ions products from BG dissolution and the beneficial functions of HA–CS shell on the surface of FN-GEL/BG hybrid nanofibers. These two constituents may be advantageous to mediating their activity in cellular signaling. Similarly, the nanofibrous structural stability of HA–CS-crosslinked GEL/BG hydrogels can be attributed to the strong electrostatic interactions of HA–CS shell layer which may protect NF-GEL to reduce dissolution. As described above, the joint welding at the cross points may also play an important role in improving the mechanical stability of NF-GEL/BG hybrid fibers. Meanwhile, the nanoscale BG particle in the nanofibrous network provide a high glass surface area and gradient distribution, thus leading to a very fast dissolution and subsequent high increase in ion concentrations and weak basic environment, which would be helpful for CS shell insoluble in wet wound areas. Therefore, it is reasonable to postulate the BG-incorporation and electrostatic crosslinking of HA–CS pairs are not only favorable for improving the thermal and mechanical integrity of NF-GEL hydrogel in wet state, but also endow the improved bioactive potential for wound healing.

4. Conclusion

We have developed a phase separation and electrostatic crosslink method to fabricate BG-incorporated, core–shell-structured nanofibrous polypeptide–polysaccharide composite systems. The oppositely charged HA–CS shell layers markedly improve the thermal and structural stability of nanofibous 3D GEL network. The inorganic ion release from BG dissolution endows bioactive and antibacterial properties of the systems. The whole manufacturing process does not involve any enivronmentally/biologicall harmful additives and the products involve no inert constituents. Therefore, this unique composition–structure relationship makes NF-GEL/BG@HA–CS hydrogels more attractive candidates for potential uses as wound-healing accelerator in many chronic, nonhealing skin wound areas.

Acknowledgements

This work is supported by National Science Foundation of China (no. 51102211), Research Fund of Zhejiang Provincial Education Department (no. 2010SSA005), the Zhejiang Provincial Natural Science Foundation of China (no. Y4110169, Y4090029), MOE Key Laboratory of Macromolecular Synthesis and Functionalization, Zhejiang University (2011MSF08), Shaoxing Science and Technology Bureau Foundation (no. SX2012-0015) and the main international project of Zhejiang province of China (no. 2009c14017).

References

Ali, S. W., Rajendran, S., & Joshi, M. (2011). Synthesis and characterization of chitosan and silver loaded chitosan nanoparticles for bioactive polyester. *Carbohydrate Polymers*, *83*, 438–446.

Boatenog, J. S., Matthews, K. H., Stevens, H. N. E., & Eccleston, G. M. (2008). Wound healing dressings and drug delivery systems: A review. *Journal of Pharmaceutical Sciences*, *97*, 2892–2899.

Brem, H., Tomic-Canic, M., Tarnovskaya, A., Ehrlich, H. P., Baskin-Bey, E., Gill, K., Carasa, M., Weinberger, S., Entero, H., & Vladeck, B. (2003). Healing of elderly patients with diabetic foot ulcers, venous stasis ulcers, and pressure ulcers. *Surgical Technology International*, *11*, 161–169.

Burdick, J. A., & Prestwich, G. D. (2011). Hyaluronic acid hydrogels for biomedical applications. *Advanced Materials*, *43*, H41–H56.

Chang, W. H., Chang, Y., Lai, P. H., & Sung, H. W. (2003). A genipin-crosslinked gelatin membrane as wound-dressing material: In vitro and in vivo studies. *Journal of Biomaterials Science: Polymer Edition*, *14*, 481–495.

Chen, Q.-Z., & Thouas, G. A. (2011). Fabrication and characterization of sol–gel derived 45S5 Bioglass®–ceramic scaffolds. *Acta Biomaterialia*, *7*, 3616–3623.

Chopra, I. (2009). The inceasing use of silver-based products as antimicrobial agents: A useful development or a cause for concern? *Journal of Antimicrobial Chemotherapy*, *59*, 587.

Ehrenreich, M., & Ruszczak, Z. (2006). Update on the tissue-engineered biological dressings. *Tissue Engineering*, *12*, 2407–2424.

Fujikawa, S., Fukui, Y., & Koga, K. (1987). Structure of genipocyanin G, a spontaneous reaction product between genipin and glycine. *Tetrahedron Letters*, *28*, 4699–4703.

Gillette, R. L., Swaim, S. F., Sartin, E. A., Bradley, D. M., & Coolman, S. L. (2011). Effects of a bioactive glass on healing of closed skin wounds in dogs. *American Journal of Veterinary Research*, *62*, 1149–1156.

Gorustovich, A. A., Perio, C., Roether, J. A., & Boccaccini, A. R. (2010). Effect of bioactive glasses on angiogenesis: A review of in vitro and in vivo evidence. *Tissue Engineering B: Review*, *16*, 199–210.

Guo, J., Leung, G., Su, H., Yuan, Q., Wang, L., Chu, T.-H., Zhang, W., Pu, J. K. S., Ng, G. K. P., Wong, W. M., Dai, X., & Wu, W. (2009). Self-assembling peptide nanofiber scaffold promotes the reconstruction of acutely injured brain. *Nanomedicine: Nanotechnology, Biology and Medicine*, *5*, 345–351.

Gurtner, G. C., Werner, S., Barrandon, Y., & Longaker, M. T. (2008). Wound repair and regeneration. *Nature*, *453*, 314.

Hartgerink, D. J., Elia, B., & Stupp, S. I. (2002). Peptide-amphiphile nanofibers: A versatile scaffold for the preparation of self-assembling materials. *Proceedings of the National Academy of Sciences of the United States of America*, *99*, 5133–5136.

Hench, L. L. (2006). The story of Bioglass®. *Journal of Materials Science, Materials in Medicine*, *17*, 967–972.

Jonker, A. M., Lowik, D. W. P. M., & van Hest, J. C. M. (2012). Peptide- and protein-based hydrogels. *Chemistry of Materials*, *24*, 759–773.

Kawai, K., Larson, B. J., Ishise, H., Carre, A. L., Nishimoto, S., Longaker, M., & Lorenz, H. P. (2011). Calcium-based nanoparticles accelerate skin wound healing. *PloS ONE*, *6*, e27106.

Lansdown, A. B. (2002). Calcium: A potential central regulator in wound healing in the skin. *Wound Repair Regeneration*, *10*, 271.

Leaper, D. J. (2006). Silver dressings: Their role in wound management. *International Wound of Journal*, *3*, 282–294.

Lewis, R., Whitting, P., ter Riet, G., O'Meara, S., & Glanville, J. (2001). A rapid and systematic review of the clinical effectiveness and cost-effectiveness of debriding agents in treating surgical wounds healing by secondary intention. *Health Technology Assessment*, *5*, 1–131.

Liang, H.-C., Chang, W.-H., Liang, H.-F., Lee, M.-H., & Sung, H.-W. (2004). Crosslinking structures of gelatin hydrogels crosslinked with genipin or a water-soluble carbodiimide. *Journal of Applied Polymers Science*, *91*, 4017–4022.

Li, J., He, A., Han, C. C., Fang, D., Hsiao, B. S., & Chu, B. (2006). Electrospinning of hyaluronic acid (HA) and HA/gelatin blends. *Macromolecule Rapid Communications*, *27*, 114–120.

Motta, G. J. (1989). Calcium alginate topical wound dressing: A new dimension in the cost-effective treatment for exudating dermal wounds and pressure sores. *Ostomy Wound Management*, *25*, 52.

Muzzarelli, R. A. A. (2009). Chitins and chitosans for the repair of wounded skin, nerve, cartilage and bone. *Carbohydrate Polymers*, *76*, 167–182.

Neel, A. E. A., Ahmed, I., Pratten, J., Nazhat, S. N., & Knowles, J. C. (2005). Characterization of antibacterial copper releasing degradable phosphate glass fibres. *Biomaterials*, *26*, 2247–2254.

Rahaman, M. N., Day, D. E., Bal, B. S., Fu, Q., Jung, S. B., Bonewald, L. F., & Tomsia, A. P. (2011). Bioactive glass in tissue engineering. *Acta Bioamterialia*, *7*, 2355–2364.

Rujitanaroj, P.-O., Pimpha, N., & Supaphol, P. (2008). Wound-dressing materials with antibacterial activity from electrospun gelatin fiber mats containing silver nanoparticles. *Polymer*, *29*, 4723.

Schneider, A., Garlick, J. A., & Egles, C. (2008). Self-assembling peptide nanofiber scaffolds accelerate wound healing. *PLoS ONE*, *1*, e1410–e1418.

Sung, H. W., Huang, D. M., Chang, W. H., Huang, R. N., & Hsu, J. C. (1999). Evaluation of gelatin hydrogel crosslinked with various crosslinking agents as bioadhesives: In vitro study. *Journal of Biomedical Materials Research*, *46*, 520–528.

Sun, G., Zhang, X., Shen, Y.-I., Sebastian, R., Dickinson, L. E., Fox-Talbot, K., Reinblatt, M., Steenbergen, C., Harmon, J. W., & Gerecht, S. (2011). Dextran hydrogel scaffolds enhance angiogenic responses and promote complete skin regeneration during burn wound healing. *Proceedings of the National Academy of Sciences of the United States of America*, *108*, 20976.

Tanaka, Y., Gong, J., & Osada, Y. (2005). Novel hydrogels with excellent mechanical performance. *Progress in Polymer Science*, *30*, 1–9.

Tchemtchoua, V. T., Atanasova, G., Aqil, A., Fileĭe, P., Garbacki, N., Vanhooteghem, O., Deroanne, C., Noel, A., Jeĭrome, C., Nusgens, B., Poumay, Y., & Colige, A. (2011). Development of a chitosan nanofibrillar scaffold for skin repair and regeneration. *Biomacromolecules*, *12*, 3194–3204.

Tran, N. Q., Joung, Y. K., Lih, E., & Park, K. D. (2011). In situ forming and rutin-releasing chitosan hydrogels as injectable dressings for dermal wound healing. *Biomacromolecules*, *12*, 2872–2878.

Uppal, R., Ramaswamy, G. N., Arnold, C., Goodband, R., & Wang, Y. (2011). Hyaluronic acid nanofiber wound dressing—production, characterization, and in vivo behavior. *Journal of Biomedical Materials Research, Part B: Applied Biomaterials*, *97B*, 20–29.

Van Vlierberghe, S., Dubruel, P., & Schacht, E. (2011). Biopolymer-based hydrogels as scaffolds for tissue engineering applications: A review. *Biomacromolecules*, *12*, 1387.

Waltimo, T., Brunner, T. J., Vollenweider, M., Stark, W. J., & Zehnder, M. (2007). Antimicrobial effect of nanometric bioactive glass 45S5. *Journal of Dental Research*, *86*, 754–757.

Wilson, J., Pigott, G. H., Schoen, F. J., & Hench, L. L. (1981). Toxicology and biocompatibility of bioglasses. *Journal of Biomedical Materials Research*, *15*, 805–815.

Xie, J., Li, X., & Xia, Y. (2008). Putting electrospun nanofibers to work for biomedical research. *Macromolecule Rapid Communications*, *29*, 1775-1192.

Xie, Z.-P., Zhang, C.-Q., Yi, C.-Q., Qiu, J.-J., Wang, J.-Q., & Zhou, J. (2009). In vivo study effect of particulate Bioglass® in the prevention of infection in open fracture fixation. *Journal of Biomedical Materials Research, Part B: Applied Biomaterials*, *90B*, 195–203.

Xu, X., & Zhou, M. (2008). Antibacterial gelatin nanofibers containing silver nanoparticles. *Fibers Polymers*, *9*, 685.

Youk, J. H., Lee, T. S., & Park, W. H. (2004). Preparation of antimicrobial ultrafine cellulose acetate fibers with silver nanoparticles. *Macromolecule Rapid Communications*, *25*, 1632–1637.

Zhang, D., Leppäranta, O., Munukka, E., Ylänen, H., Viljanen, M. K., Eerola, E., Hupa, M., & Hupa, L. (2010). Antibacterial effects and dissolution behavior of six bioactive glasses. *Journal of Biomedical Materials Research*, *93A*, 475.

Zhang, S., Gelain, F., & Zhao, X. (2005). Designer self-assembling peptide nanofiber scaffolds for 3D tissue cell cultures. *Seminar Cancer Biology*, *15*, 413–420.